

# Ram pressure stripping of disc galaxies: The role of the inclination angle

Elke Roediger\* and Marcus Brüggen\*

*International University Bremen, P.O. Box 750 561, 28725 Bremen, Germany*

Accepted. Received; in original form

## ABSTRACT

We present 3D hydrodynamical simulations of ram pressure stripping of massive disc galaxies in clusters. Studies of galaxies that move face-on have predicted that in such a geometry the galaxy can lose a substantial amount of its interstellar medium. But only a small fraction of galaxies is moving face-on. Therefore, in this work we focus on a systematic study of the effect of the inclination angle between the direction of motion and the galaxy’s rotation axis.

In agreement with some previous works, we find that the inclination angle does not play a major role for the mass loss as long as the galaxy is not moving close to edge-on (inclination angle  $\lesssim 60^\circ$ ). We can predict this behaviour by extending Gunn & Gott’s estimate of the stripping radius, which is valid for face-on geometries, to moderate inclinations.

The inclination plays a role as long as the ram pressure is comparable to pressures in the galactic plane, which can span two orders of magnitude. For very strong ram pressures, the disc will be stripped completely, and for very weak ram pressures, mass loss is negligible independent of inclination. We show that in non-edge-on geometries the stripping proceeds remarkably similar. A major difference between different inclinations is the degree of asymmetry introduced in the remaining gas disc.

We demonstrate that the tail of gas stripped from the galaxy does not necessarily point in a direction opposite to the galaxy’s direction of motion. Therefore, the observation of a galaxy’s gas tail may be misleading about the galaxy’s direction of motion.

**Key words:** galaxies: spiral – galaxies: evolution – galaxies: ISM – galaxies clusters: general

## 1 INTRODUCTION

Galaxies populate different environments, ranging from isolated field galaxies to dense galaxy clusters. Comparative observations between field and cluster galaxies reveal that, in addition to internal processes, the environment plays an important role in galaxy evolution. Disc galaxies are especially affected. Many well-known differences between cluster and field disc galaxy populations are attributed to a smaller gas content of cluster members. Such differences are the higher fraction of red galaxies and early-type galaxies in clusters (e.g. Goto et al. 2003; Pimbblet 2003) as well as the HI-deficiency of cluster disc galaxies (Cayatte et al. 1990, 1994; Solanes et al. 2001) and the reduced star formation rates (Koopmann & Kenney 1998, 2004a,b; Koopmann et al. 2005).

Several processes have been proposed to explain these features. One idea are tidal interactions between cluster members. Although the interaction timescales in clusters are rather short due to the high velocity dispersion of cluster galaxies, Moore et al. (1996,1998,1999) have shown that repeated short interactions (harassment) can have a substantial influence on cluster galaxies (see also review by Mihos 2004 and references therein). Another process is ram pressure stripping, which is the interaction between the galactic gas disc and the intracluster medium (ICM). As galaxies move through the ICM, the ram pressure is expected to push out (parts of) their interstellar medium (ISM), provided the ram pressure is strong enough. This process does not affect the dynamics of the stellar and dark matter components of the galaxy. If ram pressure stripping plays a role, one expects to find galaxies with undisturbed stellar discs and distorted and truncated gaseous discs. Such examples have been observed e.g. NGC 4522 (Kenney & Koopmann 1999, 2001; Kenney et al. 2004, Vollmer et al. 2004), NGC

\* E-mail: e.roediger@iu-bremen.de (ER); m.brueggen@iu-bremen.de (MB)

4548 (Vollmer et al. 1999) and NGC 4848 (Vollmer et al. 2001).

The ICM-ISM interaction is a complex process influenced by many parameters. Different aspects have been studied by several groups. Schulz & Struck (2001), Marcolini et al. (2003) and Roediger & Hensler (2005) showed that the ICM-ISM interaction is a multi-stage process. The most important phases are the instantaneous stripping, on a timescale of a few 10 Myr, an intermediate phase, on a timescale of up to a few 100 Myr, and a continuous stripping phase that, in principle, could continue until all gas is lost from the galaxy. Instantaneous stripping is the immediate consequence of the ram pressure dislocating the gas disc. However, the gas does not become unbound from the galactic potential immediately. It takes the intermediate phase until all displaced gas is truly lost. Schulz & Struck (2001) described this as a “hang-up” phase where gas lingers behind the disc. The continuous stripping is caused by the Kelvin-Helmholtz (KH) instability induced by the ICM wind flowing over the surface of the remaining gas disc, leading to a slow but continuous gas loss. This process is also termed turbulent/viscous stripping (see e.g. Nulsen 1982; Quilis et al. 2000).

A list of parameters that influence ram pressure stripping includes the ICM wind density,  $\rho_{\text{ICM}}$ , wind velocity,  $v_{\text{ICM}}$ , the inclination angle,  $i$ , between the disc’s rotation axis and the wind direction, the overall galaxy mass (its potential depth) and its gas mass, the variability of the ICM wind, the structure of the ISM gas disc. Gunn & Gott (1972) proposed that for galaxies moving face-on through the ICM the success or failure of ram pressure stripping can be predicted by comparing the ram pressure with the galactic gravitational restoring force per unit area. If this comparison is done for each galactic radius, a stripping radius can be estimated. In general, numerical simulations agree with this analytical estimate. For inclined geometries, no clear picture has yet emerged. In SPH simulations, Abadi et al. (1999) found a good agreement with the analytical estimate for face-on cases. For the few inclined cases they studied, their model galaxies lost significantly less gas. However, this result may be biased by their short runtime of  $\sim 100$  Myr. Using an SPH code, Schulz & Struck (2001) studied the phases of the ICM-ISM interaction in detail. They focused on face-on geometries, but also performed a few simulations with inclined galaxies. They found that inclined galaxies are stripped on longer timescales. They also studied the loss of angular momentum and found that inclined galaxies are “annealed” by a stronger loss of angular momentum. Hence, the galaxies contract and thus become more resistant against stripping. Quilis et al. (2000) used a hydrodynamical grid code to study, both, the influence of the inclination angle and an inhomogeneous gas disc structure. In their work, they concentrated on rather high ram pressures, for which they found the inclination angle to play a minor role as long as the galaxy is not moving strictly edge-on. So far the work of Vollmer et al. (2001) is the only study of the effect of a time-dependent ram pressure, as it would be the case for galaxies orbiting in clusters. Using a sticky particle code, they modelled the ram pressure as an additional variable force on the gas disc particles. They observed a significant backfall of material that had been stripped during the time of maximum ram pres-

sure but was not unbound. This is in agreement with the result of Schulz & Struck (2001) and Roediger & Hensler (2005) that even for a constant ICM wind the unbinding of stripped material takes a few 100 Myr. The sticky particle code of Vollmer et al. (2001) cannot model hydrodynamical processes such as the continuous stripping found with hydro-codes because it cannot simulate hydrodynamical instabilities. Nonetheless, this model has been applied successfully to individual galaxies (e.g. Vollmer et al. 2000, 2001, 1999; Vollmer 2003). Marcolini et al. (2003) studied ram pressure stripping of discy dwarf galaxies in groups, where the ram pressure is lower than in clusters. They used a hydrodynamical 3D grid code and studied inclinations of  $0^\circ$ ,  $45^\circ$  and  $90^\circ$ . This group found that in dwarf galaxies the inclination angle only plays a role as long as the central disc pressure is comparable to the ram pressure. While for smaller ram pressures little gas is lost, for stronger ram pressures the complete disc is stripped. Even in the range where inclination plays a role, the  $45^\circ$  runs were similar to the face-on cases and only edge-on cases could retain more gas. Roediger & Hensler (2005) presented a comprehensive parameter study of face-on stripping. They varied wind density and velocity and covered conditions from cluster centres to outskirts and galaxy groups. The ram pressure,  $p_{\text{ram}} = \rho_{\text{ICM}} v_{\text{ICM}}^2$ , depends on, both, ICM density and velocity, and usually it is assumed the stripping depends on  $p_{\text{ram}}$ , and not on  $\rho_{\text{ICM}}$  and  $v_{\text{ICM}}$  individually. While this was confirmed in general by Roediger & Hensler (2005), they found that supersonic runs tend to suffer slightly less than corresponding subsonic runs. This work used a 2D hydrodynamical grid code and was thus restricted to the face-on geometry.

Even though ram pressure stripping has been studied by several groups, most simulations were performed for a face-on geometry, either because the code was 2D or because this geometry is expected to show the strongest impact. Qualitative results for the influence of the inclination angle have been found, but they do not agree in all points. So here, we concentrate on the influence of the inclination angle in the case of massive galaxies and present 3D hydrodynamical simulations that were performed with the adaptive-mesh-refinement code FLASH. We study the amount of gas loss and discuss asymmetrical structures introduced in the remaining gas disc. We also present projected gas surface density maps which reveal interesting implications for the interpretation of observational data.

In Sect. 2, we briefly introduce the code and describe our galaxy model and simulation parameters. In Sect. 3, we discuss some analytical considerations, and in Sect. 4 we present our simulation results. Finally, in Sect. 5 we compare our results to previous work and discuss their implications.

## 2 METHOD

We study the motion of the galaxy through the cluster in the rest frame of the galaxy. Therefore, its motion translates into an ICM wind flowing past the galaxy.

## 2.1 Code

The simulations were performed with the FLASH code (Fryxell et al. 2000), a hydrodynamical adaptive-mesh-refinement code with a PPM hydro solver. All boundaries but the inflow boundary are open. The simulations presented here are performed in 3D. We use a simulation box of size of  $(x_{\min}, x_{\max}) \times (y_{\min}, y_{\max}) \times (z_{\min}, z_{\max}) = (-64.8 \text{ kpc}, 64.8 \text{ kpc})^3$ . For the low ram pressure runs a box size of  $(x_{\min}, x_{\max}) \times (y_{\min}, y_{\max}) \times (z_{\min}, z_{\max}) = (-97.2 \text{ kpc}, 97.2 \text{ kpc}) \times (-64.8 \text{ kpc}, 64.8 \text{ kpc}) \times (-97.2 \text{ kpc}, 97.2 \text{ kpc})$  was used to prevent interference with the boundaries. The galactic centre is located at  $(x_{\text{gal}}, y_{\text{gal}}, z_{\text{gal}}) = (0, 0, 0)$ . The ICM wind is flowing along the  $y$ -axis into the positive direction. Most simulations were done using 4 refinement levels, resulting in an effective resolution of 500 pc and an effective number of grid cells of  $256^3$  ( $384^3$  for the low ram pressure runs). For comparison, we also run a few test simulations with 5 refinement levels (effective grid size of  $512^3$ , and effective resolution of 250 pc) (see Appendix A). The refinement criteria were the standard density and pressure gradient criteria.

In the FLASH code, we used a mass scalar to “dye” the galactic gas. Thus, we can identify which fraction of gas inside a grid cell originated from the galactic disc (for a more detailed description of such “dyeing” techniques see Roediger & Hensler 2005).

## 2.2 Model galaxy

We model a massive spiral galaxy with a flat rotation curve at  $200 \text{ km s}^{-1}$ . It consists of a gas disc, a stellar disc, a stellar bulge and a dark matter (DM) halo. For the gravitational potential of the stellar disc, bulge and DM halo we use the following analytical descriptions:

Stellar disc: Plummer-Kuzmin disc, see Miyamoto & Nagai (1975) or Binney & Tremaine (1987). Such discs are characterised by their mass,  $M_*$ , and radial and vertical scale lengths,  $a_*$  and  $b_*$ , respectively.

Stellar bulge: Spherical Hernquist bulge (see Hernquist 1993). In case of a spherical bulge, the gravitational potential,  $\Phi$ , depends on radius,  $r$ , as  $\Phi(r) = -\frac{GM_{\text{bulge}}}{r+r_{\text{bulge}}}$ , where  $M_{\text{bulge}}$  is the mass of the bulge,  $r_{\text{bulge}}$  the scale radius and  $r$  the spherical radius.

DM halo: The spherical model of Burkert (1995), including the self-scaling relations, i.e. the DM halo is characterised by the radial scale length  $r_{\text{DM}}$  alone. For the equation of the analytical potential see also Mori & Burkert (2000).

The self-gravity of the gas is neglected as the gas contributes only a small fraction to the overall galactic mass. The galaxy model parameters are summarised in Table 1. In order to prevent steep density gradients in the galactic plane and in the galactic centre, the gas disc is described by a softened exponential disc :

$$\rho(R, Z) = \frac{M_{\text{gas}}}{2\pi a_{\text{gas}}^2 b_{\text{gas}}} 0.5^2 \operatorname{sech}\left(\frac{R}{a_{\text{gas}}}\right) \operatorname{sech}\left(\frac{|Z|}{b_{\text{gas}}}\right). \quad (1)$$

The coordinates  $(R, Z)$  are galactic cylindrical coordinates. The radial and vertical scale lengths are  $a_{\text{gas}}$  and  $b_{\text{gas}}$ , respectively. For  $R \gtrsim a_{\text{gas}}$  and  $|Z| \gtrsim b_{\text{gas}}$ , this density distribution converges towards the usual exponential disc

Table 1. Galaxy model parameters.

stellar disc	$M_*$	$10^{11} M_{\odot}$
	$a_*$	4 kpc
	$b_*$	0.25 kpc
bulge	$M_{\text{bulge}}$	$10^{10} M_{\odot}$
	$r_{\text{bulge}}$	0.4 kpc
DM halo	$r_{\text{DM}}$	23 kpc
gas disc	$M_{\text{gas}}$	$10^{10} M_{\odot}$
	$a_{\text{gas}}$	7 kpc
	$b_{\text{gas}}$	0.4 kpc
	$v_{\text{rot}}$	$200 \text{ km s}^{-1}$

$\rho(R, Z) = \frac{M_{\text{gas}}}{2\pi a_{\text{gas}}^2 b_{\text{gas}}} \exp(-R/a_{\text{gas}}) \exp(-|Z|/b_{\text{gas}})$ . For the corresponding exponential disc,  $M_{\text{gas}}$  is the total gas mass. We chose  $M_{\text{gas}}$  such that in the outer regions the gas disc converges to an exponential gas disc with 10% of the stellar disc mass, i.e.  $M_{\text{gas}} = 0.1M_*$ . Due to the reduction of the gas density in the central part of the softened exponential disc, the integrated gas mass amounts to  $6 \cdot 10^9 M_{\odot}$ . Given the density distribution in the disc, its pressure and temperature distribution are set such that hydrostatic equilibrium with the ICM is maintained in the direction perpendicular to the disc plane. In radial direction, the disc’s rotation velocity is set so that the centrifugal force balances the gravitational force and pressure gradients. We have cut the gas disc smoothly to a finite radius of 26 kpc to prevent interaction of stripped gas with the grid boundaries. This smooth cutting was achieved by multiplying the gas density distribution  $\rho(R, Z)$  with  $0.5(1 + \cos(\pi(R - 20 \text{ kpc})/6 \text{ kpc}))$  for  $20 \text{ kpc} < R \leq 26 \text{ kpc}$ . Figure 1 shows radial profiles of density, surface density, pressure and rotation velocity for the initial model.

We measure the inclination angle,  $i$ , of the galaxy as the angle between its rotation axis and the ICM wind direction. Thus  $0^\circ$  corresponds to a face-on motion of the galaxy, and  $90^\circ$  to edge-on.

## 2.3 ICM conditions

In order to study the influence of the inclination angle,  $i$ , isolatedly, we use a constant ICM wind. The additional effect of a variable ICM wind, as one would expect for a cluster passage, will be studied in a forthcoming paper.

The strength of the ICM wind is characterised by the ram pressure,  $p_{\text{ram}} = \rho_{\text{ICM}} v_{\text{ICM}}^2$ , which depends on, both, ICM wind density,  $\rho_{\text{ICM}}$ , and velocity,  $v_{\text{ICM}}$ . Roediger & Hensler (2005) have shown that the ram pressure is the relevant parameter and not  $\rho_{\text{ICM}}$  or  $v_{\text{ICM}}$ . Therefore, we use  $v_{\text{ICM}} = 800 \text{ km s}^{-1}$  for most simulations and vary the ram pressure by varying  $\rho_{\text{ICM}}$ . We chose the ICM temperature such that the sound speed is  $1000 \text{ km s}^{-1}$ . Thus, the standard  $v_{\text{ICM}}$  corresponds to a Mach number of 0.8. For comparison, a few runs with supersonic  $v_{\text{ICM}} = 2530 \text{ km s}^{-1}$  have also been performed. The parameters for  $p_{\text{ram}}$ ,  $\rho_{\text{ICM}}$ ,  $v_{\text{ICM}}$  and  $i$  are summarised in Table 2. We will refer to the three ram pressures used as low, medium and high. If not stated otherwise, we refer to runs with  $v_{\text{ICM}} = 800 \text{ km s}^{-1}$ .

We start the simulation with the ICM at rest and then

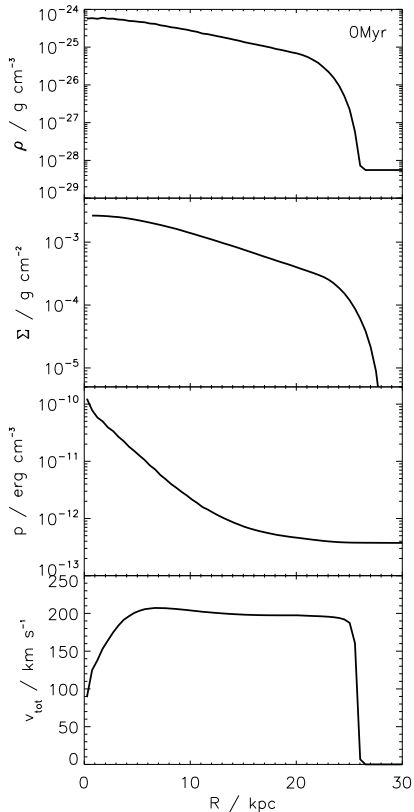


**Figure 1.** Radial profiles of the density,  $\rho$ , pressure,  $p$ , and rotation velocity,  $v_{\text{rot}}$ , in the galactic plane for the initial model. Also the radial profile for the projected ISM surface density,  $\Sigma$ , is shown.

**Table 2.** ICM wind parameters. Crosses indicate which ICM wind parameter - inclination combinations have been simulated.

$p_{\text{ram}}/$ ( $\text{erg cm}^{-3}$ )	$\rho_{\text{ICM}}/$ ( $\text{g cm}^{-3}$ )	$v_{\text{ICM}}/$ ( $\text{km s}^{-1}$ )	inclination $i/^\circ$				
			0	30	60	75	90
$6.4 \cdot 10^{-11}$	$10^{-26}$	800	×	×	×		×
$6.4 \cdot 10^{-12}$	$10^{-27}$	800	×	×	×	×	×
$6.4 \cdot 10^{-12}$	$10^{-28}$	2530		×		×	
$6.4 \cdot 10^{-13}$	$10^{-28}$	800	×	×	×		×

increase the inflow velocity over the first 50 Myr from zero to  $v_{\text{ICM}}$ .

In order to include all stages of the ICM-ISM interaction, the overall runtime of our simulations is 1 Gyr.

### 3 ANALYTICAL CONSIDERATIONS

#### 3.1 Different phases

As described in previous works, the ICM-ISM interaction proceeds in multiple phases. The discussion of the phases in Sect. 1 made clear that the overall process is quite complex. Analytical estimates exist mainly for the instantaneous stripping phase in face-on geometry (see Sect. 3.2). Marcolini et al. (2003) estimated a stripping radius for the

edge-on geometry by assuming that the instantaneous stripping can be neglected and the stripping radius will be set by the KH-instability. They estimated the radius up to which the galaxy's gravity can suppress the KH-instability, and assumed that gas outside this radius will be stripped. They found that, both, the estimates for face-on and edge-on cases are rather similar. However, the timescale for the continuous stripping, which is the relevant process in the edge-on geometry, operates on a much longer timescale. Roediger & Hensler (2005) estimated that the mass loss rate during the continuous stripping phase is of the order of  $1M_{\odot}/\text{yr}$ .

In the following sections, we discuss the estimate for the stripping radius in the instantaneous stripping phase and try to derive an estimate for inclined geometries.

#### 3.2 Face-on geometry

The usual way to estimate the amount of gas loss during the instantaneous stripping phase for galaxies moving face-on through the ICM follows the suggestion of Gunn & Gott (1972). Here, one compares the gravitational restoring force per unit area and the ram pressure for each radius of the galaxy. At radii where the restoring force is larger, the gas can be retained, at radii where the ram pressure is larger, the gas will be stripped. The transition radius is called the stripping radius. In order to calculate the restoring force per unit area, it is assumed that the gas disc can be approximated by an infinitely thin disc. Then, the restoring force per unit area would be

$$f_{\text{grav}}(R) = \Sigma_{\text{gas}}(R) \frac{\partial \Phi}{\partial Z}(R), \quad (2)$$

where  $\Phi$  is the gravitational potential of the galaxy and  $\Sigma_{\text{gas}}(R)$  the gas surface density. As pointed out by e.g. Roediger & Hensler (2005), the gradient of  $\partial \Phi / \partial Z$  exactly in the disc plane is zero, so if  $\partial \Phi / \partial Z$  exactly in the galactic plane is used, this estimate would not yield any restoring force. In order to obtain a reasonable estimate, one can use the maximum gradient  $\frac{\partial \Phi}{\partial z}(R, Z)$  behind the disc plane at a given  $R$ . In general, the resulting stripping radii and retained gas masses from numerical simulations agree well with the predictions from this simple estimate.

#### 3.3 Inclined cases

Now we wish to move on from face-on geometries to inclined cases. As in face-on geometries, we assume that the gas disc can be described by an infinitely thin disc. For a given surface element  $dA$  at radius  $R$  in the galactic plane, the ram pressure force is  $\rho_{\text{ICM}} v_{\text{ICM}}^2 \cos i dA$ , because we have to use the projected cross-section of this surface element. This force is axisymmetrical with respect to the galactic rotation axis for all  $i$ . We can also interpret this force in terms of an *effective* inclination-dependent ram pressure  $\cos i \rho_{\text{ICM}} v_{\text{ICM}}^2$ . Clearly, the ram pressure force decreases with inclination. In addition to the reduced ram pressure force, also the correct gravitational restoring force needs to be calculated. For a surface element  $dA$  in the galactic plane at galactic radius  $R$  and azimuthal angle  $\phi$ , the restoring force is the projection of the sum of local gravitational force and centrifugal force onto wind direction. Since the centrifugal force

and the radial gravitational force in a disc galaxy balance, we can drop both terms from our analysis. Only the projection of the gravitational force perpendicular to the disc plane onto wind direction remains. This is  $\cos i \cdot f_{\text{grav}} dA$  with  $f_{\text{grav}}$  calculated as in Eqn. 2. Again, this force is axisymmetrical with respect to the galactic rotation axis. If now the ram pressure force and the restoring force are compared for all disc radii, the factor  $\cos i$  drops out completely. Consequently, the stripping radius should be independent of inclination. One of the assumptions for this estimate is that the gas disc can be approximated by an infinitely thin disc. Clearly, this assumption is not valid for highly inclined cases, so the estimate is expected to fail for near-edge-on cases. However, for moderate inclinations it could give a useful approximation. For near-edge-on inclinations, we expect that the galaxy loses less gas.

## 4 SIMULATION RESULTS

The most striking result of our simulations is that with increasing inclination a stronger and stronger degree of asymmetry is introduced to the gas disc. This asymmetry makes simple concepts such as a stripping radius difficult to apply.

### 4.1 Snapshots of the evolution

To visualise the 3D data, we show slices through the simulation box and projected gas densities. Figures 2 and 3 display the local gas density in certain planes through the galaxy for an inclination of  $30^\circ$  (Fig. 2) and  $90^\circ$  (Fig. 3). Both plots represent runs with medium ram pressure. Snapshots at 3 different times are shown. For the  $30^\circ$  case, the disc remains rather symmetrical, whereas especially early snapshots of the  $90^\circ$  case display a strong degree of asymmetry.

In Figs. 4, 5 and 6, we show projected gas densities at several timesteps for the same runs as in Figs. 2 and 3, but also for the corresponding  $60^\circ$  run. For all three runs, we show projections along the three coordinate axes. Only galactic gas (identified by its ‘‘colour’’, see Sect. 2.1) is shown.

The snapshots reveal an interesting trend: At early times a higher inclination causes stronger asymmetry: one side (roughly the upstream side) is stripped more strongly than the other. Details of how the rotation of the disc affects the stripping are discussed below. However, even for the edge-on case, the asymmetry decreases with time and the remaining gas disc becomes circular again. This is caused by the rotation of the gas disc. At a galactic radius of 10 kpc, the rotation time is roughly 300 Myr, so in the course of our simulation the disc rotates roughly 3 times. Therefore, for the case of a constant ICM wind, eventually each part of the disc passes the region of strongest stripping, and the disc becomes symmetrical again.

### 4.2 Velocity information

Vollmer et al. (2001) stressed that velocity information is crucial for the correct interpretation of HI observations of ram pressure stripped galaxies. Due to the fact that we have used a constant ICM wind, the velocity structure of the stripped material reflects mainly the superposition of

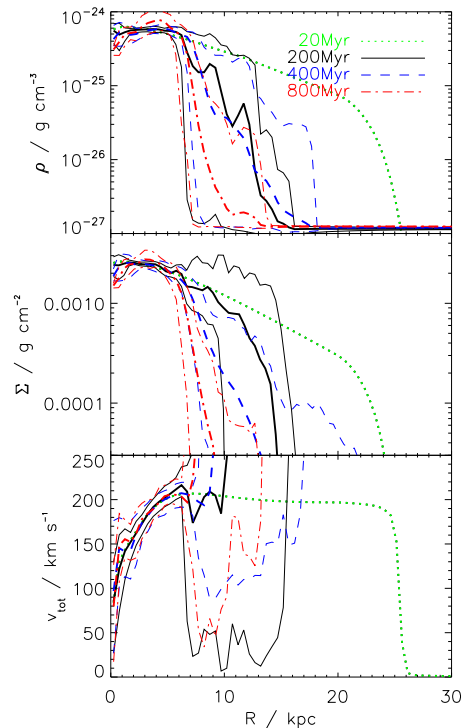


**Figure 7.** Evolution of radial profiles, for density,  $\rho$ , and rotation velocity,  $v_{\text{rot}}$ , in the galactic plane. Also the projected gas surface density,  $\Sigma$ , is shown. The profiles belong to the same run as in Fig. 2. The thick line displays the mean profile averaged azimuthally over the disc, the thin lines display the minimum and maximum values for each radius. For further explanation see text, Sect. 4.3. The colours/linestyles code four different times, see legend.

the galactic rotation and the acceleration by the ICM wind. The velocity structure will be more interesting for simulations with variable ICM winds.

### 4.3 Radial profiles

In Fig. 7, we display the evolution of radial profiles. To generate this plot, we measured radial profiles along 12 radial lines that are separated by  $30^\circ$  in the galactic disc. The thick lines show the average of these profiles, the thin lines maximum and minimum value for each radius. The profiles reveal that the inner part of the gas disc remains symmetrical, whereas the outer part becomes asymmetrical.

The decrease of the central density is caused by the spatial discretisation of our grid. In grid-codes, advection of mass and momentum into non-axial directions is always accompanied by a numerical viscosity due to numerical diffusion. In the rotating gas disc, the gas has to move on circular orbits in a Cartesian grid. This geometrical mismatch is strongest in the inner part of the galaxy. Below a certain radius, the resolution of the rotational motion becomes insufficient and the numerical diffusion introduces radial velocities, which lead to a decrease of the central density. We checked in higher-resolution runs that this behaviour does not influence our results (see Appendix A).

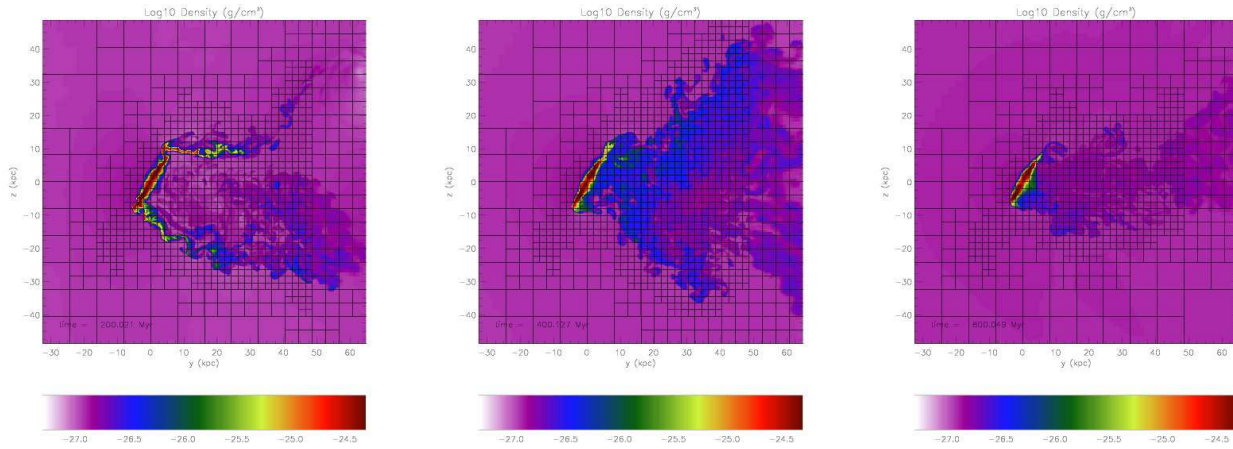


**Figure 2.** Slices in  $y$ - $z$ -plane at  $x = 0$ , colour-coded density for different timesteps. For medium ram pressure, inclination of  $30^\circ$ . The ICM wind is flowing from left to right. Also the grid structure is shown: One square is the crosssection of one block =  $8^3$  grid cells. These snapshots are taken from the run with 250 pc resolution.

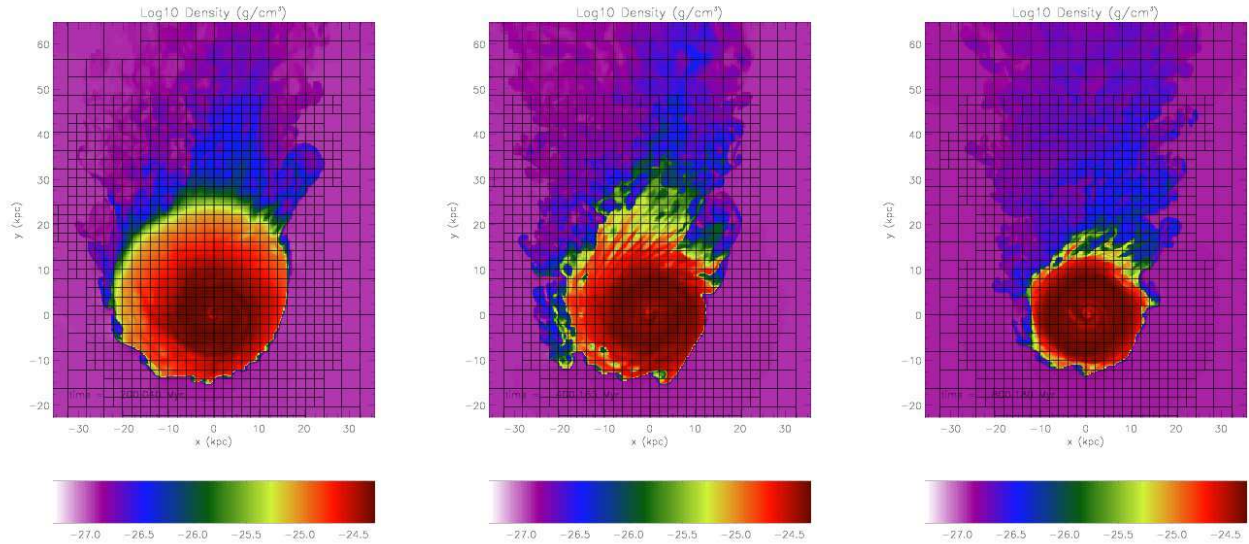


**Figure 3.** Slices in  $x$ - $y$ -plane at  $z = 0$ , colour-coded density for different timesteps. For medium ram pressure, inclination of  $90^\circ$ . The ICM wind is flowing from bottom to top. For more details see Fig. 2.

#### 4.4 Mass loss / radius decrease

##### 4.4.1 Radius and mass measurement

In the light of the previous plots, it is not clear how the radius of the gas disc should be defined. We decided to include the asymmetry in our measurement. We scan along 12 radial lines, separated by an angle of  $30^\circ$ , in the galactic plane. For each of these scan lines, we find the radius where the density drops below  $10^{-26} \text{ g cm}^{-3}$  for the first time. This is the stripping radius for this scan line. This density limit seems rather arbitrary, but Roediger (2005) tested different options and found this one to be the most appropriate and representative one. We average the results of all scan lines to obtain a mean disc radius  $R_{\text{mean}}$ , but we also compute the maximum and minimum radius  $R_{\text{max}}$  and  $R_{\text{min}}$ .

Two masses are of interest here: the mass  $M_{\text{disc}}$  of gas inside a cylinder centred on the galaxy (radius = 27 kpc, thickness =  $\pm 5$  kpc), and the mass of gas bound to the galaxy,  $M_{\text{bnd}}$ . In order to exclude the ICM in  $M_{\text{disc}}$ , we only consider gas with a temperature less than  $10^7$  K. The bound mass is given by the sum of the gas mass in all those grid cells where the total energy density  $e_{\text{therm}} + e_{\text{kin}} + e_{\text{pot}} = p/(\gamma - 1) + 0.5\rho(v_x^2 + v_y^2 + v_z^2) + \rho\Phi$  is negative.

##### 4.4.2 Radius and mass

The evolution of disc mass and radius is shown in Fig. 8. The left, middle and right plot correspond to strong, medium and weak ram pressure, the inclinations are colour-coded. The reason why the initial mass appears less in the case

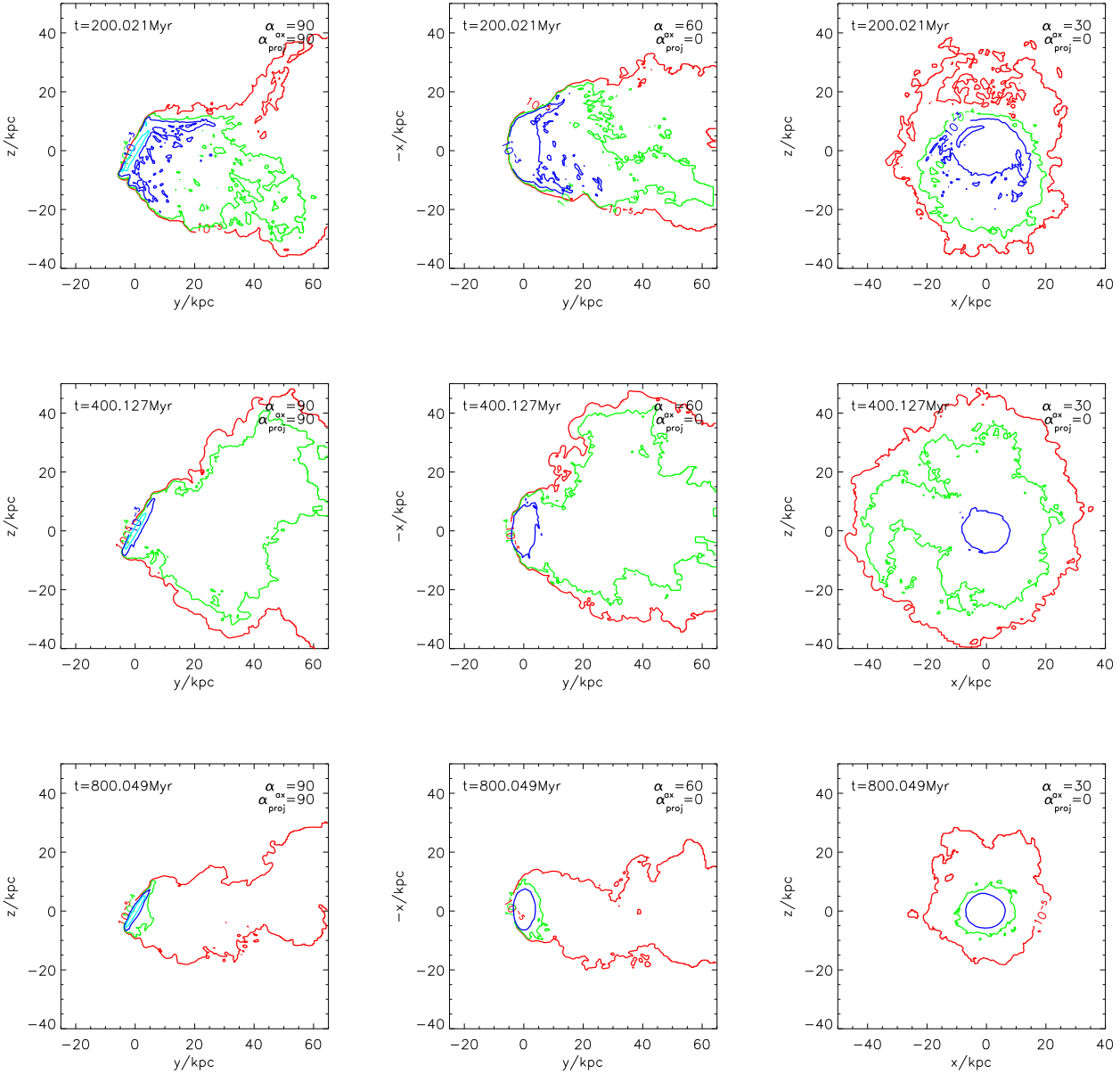


**Figure 4.** Projected gas densities along  $x$ -,  $z$ -, and  $y$ -axis in the left, middle and right column, respectively. Each row is for the same timestep that is printed in the top right corners of each panel. For medium ram pressure and inclination of  $30^\circ$ . Contour levels are  $10^{-5}, -4, -3, -2 \text{ g cm}^{-2}$ .

of the high ram pressure is that we have set the gas disc in pressure equilibrium with the ICM. For a higher  $\rho_{\text{ICM}}$  but constant ICM temperature, the ICM pressure is higher, which causes the outer layers of the gas disc to have a higher pressure. As the density distribution is fixed, this means the outer layers have a higher temperature and, therefore, drop out of our calculation of  $M_{\text{disc}}$  due to the temperature limit (see also discussion of this effect in Roediger & Hensler 2005). In order to include the asymmetry of the disc, we plot  $R_{\text{min}}(t)$  and  $R_{\text{max}}(t)$  as a function of time. In addition, we overplot the mean radius,  $R_{\text{mean}}(t)$ . For strong and medium ram pressure, it is obvious that the degree of asymmetry increases with inclination. We have also plotted the quantities

$R_{\text{max}} - R_{\text{min}}$  and  $(R_{\text{max}} - R_{\text{min}})/R_{\text{mean}}$  in Fig. 9 to quantify the degree of asymmetry.

Several interesting statements can be made from the radius and mass plots:

- Depending on ram pressure, we can strip the disc completely, partially or only marginally.
- The evolution of the retained mass and, particularly, the disc radius are remarkably similar for face-on,  $30^\circ$  and  $60^\circ$  runs. The runs for  $0^\circ$  and  $30^\circ$  are nearly indistinguishable, and in the  $60^\circ$  case only slightly less mass is lost.
- For all but the edge-on runs, we can clearly distinguish the three phases discussed in Roediger & Hensler (2005) and

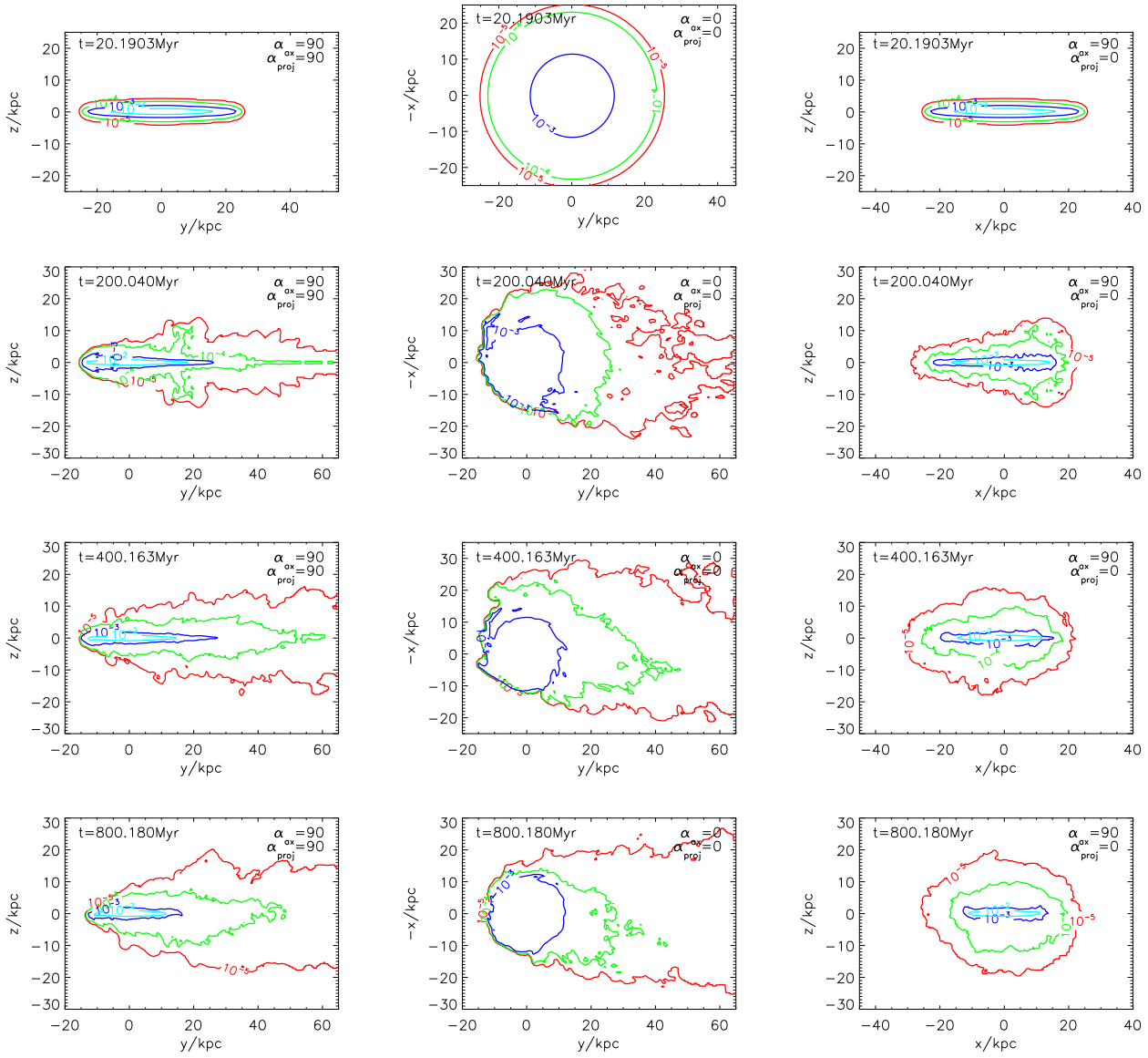


**Figure 5.** Projected gas densities along  $x$ -,  $z$ -, and  $y$ -axis. For medium ram pressure and inclination of  $90^\circ$ . See also Fig. 4.

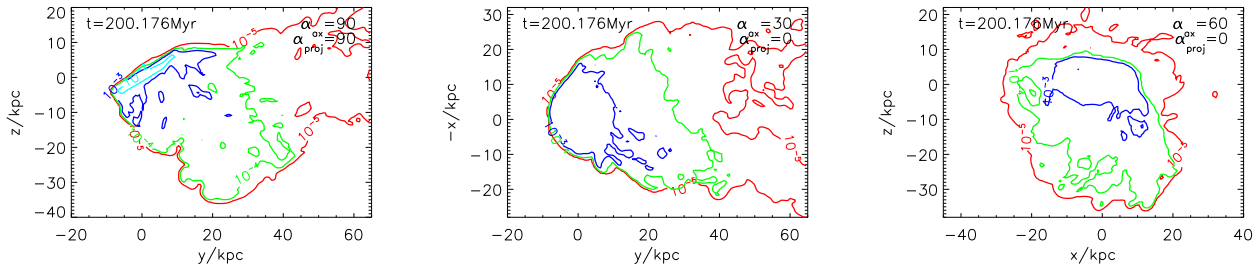


**Figure 6.** Projected gas densities along  $x$ -,  $z$ -, and  $y$ -axis. For medium ram pressure and inclination of  $60^\circ$ . See also Fig. 4.



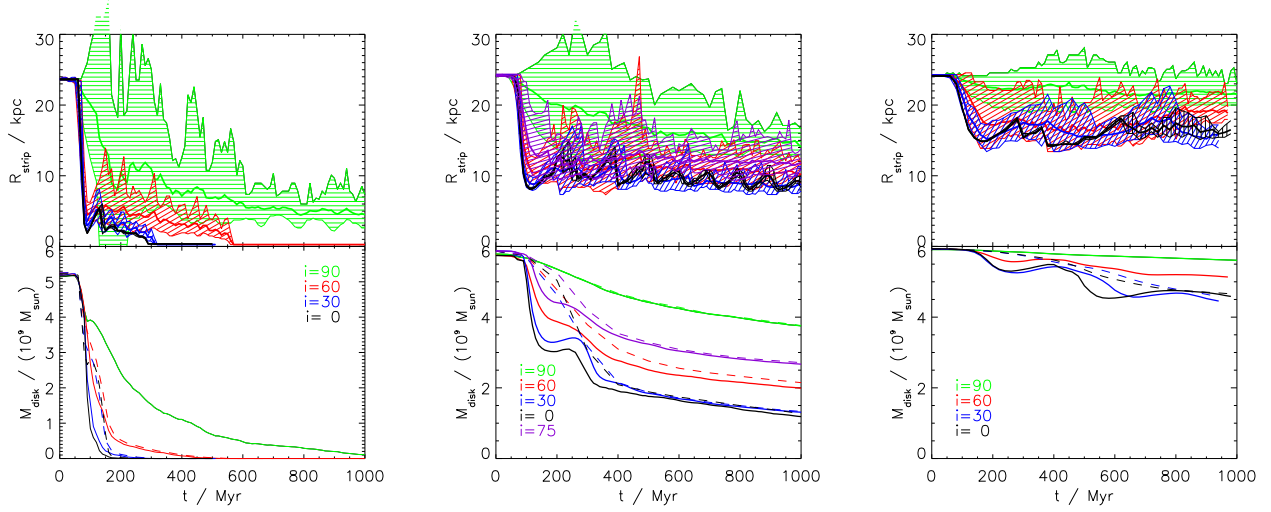


**Figure 8.** Radius and mass of the remaining gas disc for three ram pressures (left, middle and right plot correspond to strong, medium and weak ram pressure) and different inclinations (colour-coded). For the radius, we show the mean radius (thick solid line) and the minimum and maximum radius (thin lines of same colour). The area between the minimum and maximum radius curves is hatched for easier orientation. In addition to the colour, also the direction of hatching codes the inclination (e.g. horizontal hatching for edge-on). Thin dashed lines in mass plot are bound gas mass, thick solid lines are the mass in a fixed disc region (see text, Sect. 4.4.1). Both, mass and radius do not drop immediately because we switch on the flow at the inflow boundary at  $t = 0$ , and then the flow needs a certain time to reach the galaxy.

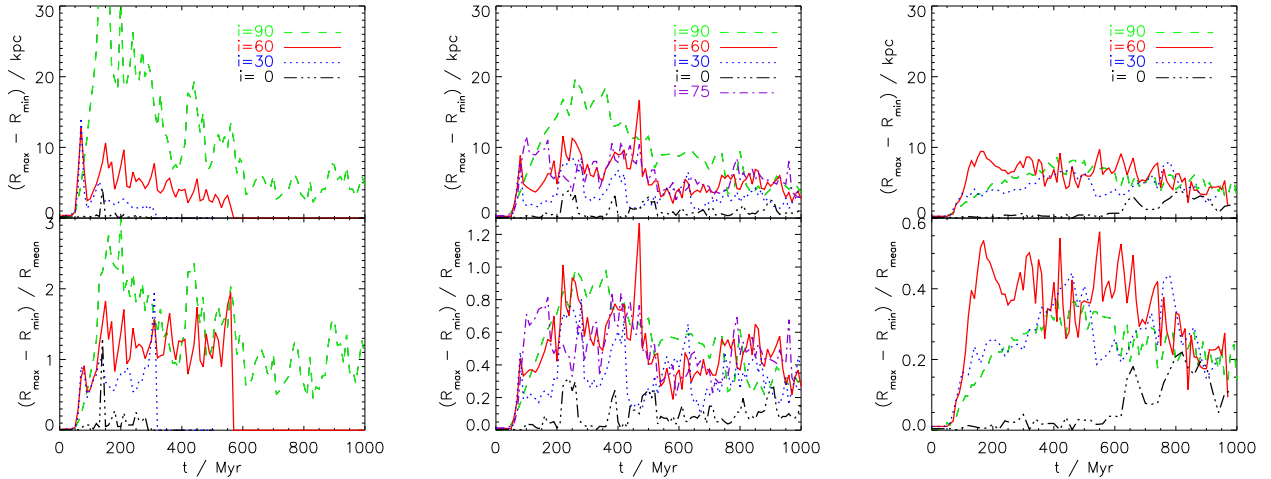


**Figure 9.** Demonstration of the asymmetry of the gas disc and its evolution. The asymmetry is shown by  $R_{\max} - R_{\min}$  in the top panels, and the same normalised to  $R_{\text{mean}}$  in the bottom panels. For three ram pressures: left, middle and right plot correspond to strong, medium and weak ram pressure. In each plot, the results for different inclinations are shown (coded by colour/linestyle, see legend). Please note the different scales on the  $y$ -axes of the bottom panels.

in Sect. 1:

The first is the instantaneous stripping phase, during which the outer part of the gas disc is pushed in the downwind direction. This phase ends with the first minimum in  $R_{\text{mean}}(t)$ . The first minimum in  $M_{\text{disc}}(t)$  appears slightly later because the gas has to leave our defined “disc region” first before it is no longer considered as disc gas.

The next phase is the intermediate phase, which is characterised by  $M_{\text{bnd}}(t) > M_{\text{disc}}$ .

Finally, the phase of continuous stripping follows.

- The durations of, both, the instantaneous stripping phase and the intermediate phase are longer for weaker ram

pressures. For a fixed  $p_{\text{ram}}$  they are independent of inclination.

- For non-edge-on cases, the evolution of  $R_{\text{mean}}$  after the instantaneous phase is slow.

- For a given  $p_{\text{ram}}$ , the mass loss rate in the continuous stripping phase seems to be independent of inclination. This feature is most relevant for medium ram pressures, where neither the mass loss is negligible (like for weak ram pressures) nor the disc is stripped completely (like for the strong ram pressure).

The basic point in all these aspects is that the stripping

process is nearly independent of inclination as long as the inclination is not close to edge-on.

The dependence of asymmetry on ram pressure and inclination is more complex. Moreover, the asymmetry decreases with time. In general, the face-on cases show nearly no asymmetry. The absolute asymmetry (i.e.  $R_{\max} - R_{\min}$ ) for the edge-on cases depends strongly on ram pressure, where higher ram pressures lead to significantly higher asymmetries. For the remaining inclinations, the absolute asymmetry is approximately independent of ram pressure. The dependence of the relative asymmetry (i.e.  $(R_{\max} - R_{\min})/R_{\text{mean}}$ ) on ram pressure reflects the dependence of  $R_{\text{mean}}$  on  $p_{\text{ram}}$ . The radial profiles in Fig. 7 reveal that the asymmetry is restricted to the outer part of the gas disc. The inner part remains symmetrical. This is even true for the medium ram pressure edge-on case, as can be seen in Fig. 3. Even for inclined cases, an inner part of the gas disc remains more or less untouched.

The comparison between subsonic and supersonic runs with identical ram pressure reveals a similar result to the result of Roediger & Hensler (2005). In the supersonic case, the galaxy can retain slightly more mass than in the subsonic case. The difference in retained masses increases with inclination. For highly inclined galaxies, also the asymmetry of the disc is temporarily larger in the supersonic case.

#### 4.5 Comparison analytical/numerical

Due to the asymmetry of the disc and the ongoing evolution, it is not straightforward to compare the numerical results to the analytical predictions. A first question to answer is at which time we have to measure mass and radius in our simulations to make a meaningful comparison to the analytical prediction. We take measurements at two timesteps: at the end of the instantaneous phase and at the end of the intermediate phase. For the strong ram pressure, the intermediate phase is finished at  $t = 175$  Myr, for the medium ram pressure at  $t = 400$  Myr, and for the weak one at  $t = 800$  Myr. Except for the edge-on cases, the stripping radius does not change during the intermediate phase. Therefore, the radius measurements taken at the end of the intermediate phase are also representative for the end of the instantaneous phase. The disc mass, however, changes during the intermediate phase. As a further complication,  $R_{\max}(t)$  and  $R_{\min}(t)$  oscillate on rather short timescales. We average these quantities over a smoothing length of 100 Myr to derive typical values.

In Fig. 10, we show the numerical results and the analytical estimate for the stripping radius and the remaining mass in the disc. The analytical estimate is displayed by the dotted lines. The predicted stripping mass given in the lower panel of this plot is simply the disc mass inside the stripping radius. For the numerical stripping radius, we show  $R_{\text{mean}}$  as diamonds and the range  $R_{\min}$  to  $R_{\max}$  as an error bar. For the mass remaining in the disc, we show the numerical results at the end of the intermediate phase as diamonds. The disc mass at the end of the instantaneous phase is shown by stars. However, for the high ram pressure case this quantity cannot be derived.

For the face-on cases ( $i = 0$ ), the analytical estimate and the numerical result for the stripping radius agree well. The same is true for the disc mass at the end of the instantane-

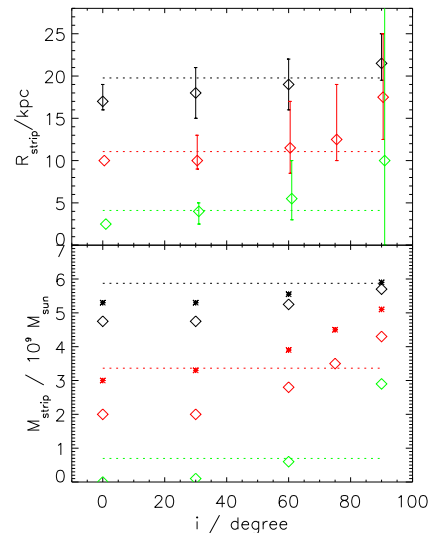


**Figure 10.** The analytical estimate of stripping radius and stripping mass as a function of inclination for three different ram pressures (black=weak, red=medium, green=strong) is shown by dotted lines. Also the numerical results are shown. We measure the numerical stripping radius and mass at the end of the intermediate phase, see text for a more detailed discussion. For the numerical radius we give the mean radius as a diamond, and the range between the minimum and maximum measured radius as an error bar. See text for further explanation (Sect. 4.5). The disc mass at the end of the intermediate phase is shown by diamonds. In addition, we plot the disc mass at the end of the instantaneous phase as stars.

neous phase. The numerical values are just slightly smaller than the predicted ones. Here we confirm the result of previous works. At the end of the intermediate phase the galaxy has already lost more than the gas outside  $R_{\text{strip}}$ . Therefore, the numerical values for the disc mass at the end of the intermediate phase are significantly lower than the analytical prediction.

For inclinations  $\lesssim 30^\circ$ , neither stripping radius nor disc mass depend on inclination. For  $30^\circ < i \lesssim 60^\circ$  the dependence on inclination is weak. Only for  $i \gtrsim 60^\circ$  the stripping radius and disc mass increase with inclination. Therefore, the simulation results confirm the prediction made in Sect. 3.3.

The mass loss rate in the continuous stripping phase is remarkably similar in all cases and is about  $1M_\odot/\text{yr}$ . This is similar to the results of Roediger & Hensler (2005).

## 5 DISCUSSION

### 5.1 The influence of the inclination

According to our simulations, the inclination angle does not affect stripping significantly unless the galaxy moves close to edge-on. This result agrees with the trends found by Quilis et al. (2000) and Marcolini et al. (2003). In contrast to Quilis et al. (2000), we do not find that only strict edge-on galaxies suffer less stripping, but we find that  $i$  affects the amount of mass loss for inclinations within  $\sim 30^\circ$  of the edge-on geometry. Moreover, we have studied the stripping

process for longer runtimes and investigated a larger range of ram pressures.

Our result disagrees with Schulz & Struck (2001) who find that inclined galaxies are stripped on a longer timescale, also for inclinations around  $45^\circ$ . In contrast, in our simulations the phases of the ICM-ISM interaction are remarkably independent of inclination. The duration of the phases is comparable to what was found by Roediger & Hensler (2005).

Vollmer et al. (2001) have included a time-dependent ram pressure in their simulations, which seems to make the influence of inclination rather messy. They could not find a correlation between ram pressure, inclination angle and stripping radius (or remaining disc diameter), but they give an empirical fit for the remaining mass. We checked whether our simulation results for the disc masses follow their suggestion, but this is not the case.

Based on their study of dwarf galaxies, Marcolini et al. (2003) argue that the inclination is only important when the ram pressure is comparable to the central pressure  $p_0$  of the galactic potential well. For  $p_{\text{ram}} > p_0$  the galaxy will be stripped completely, independent of inclination, and for  $p_{\text{ram}} < p_0$  only very little gas is lost. For our galaxy, the central pressure is  $p_0 \approx 10^{-10} \text{ erg cm}^{-3}$ . Our ram pressures are  $6.4 \cdot 10^{-11, -12, -13} \text{ erg cm}^{-3}$ . If only the central galactic pressure is compared with  $p_{\text{ram}}$ , a dependence on inclination should be prominent only in the case of our strongest ram pressure. In our simulations, however, at least the strong and the medium ram pressure case clearly depend on inclination. We suggest that not only the central disc pressure is relevant for this comparison, but the pressure profile along the galactic plane. For our model galaxy, the pressure along the galactic plane drops to about  $10^{-11} \text{ erg cm}^{-3}$  at a radius of 5 kpc and down to about  $10^{-12} \text{ erg cm}^{-3}$  at a radius of 10 kpc. This explains why the inclination plays a role for the strong and the medium ram pressure. For the weak ram pressure, our galaxy loses little mass for all inclinations. However, even there, the influence of the inclination is the same. We conclude that the result of Marcolini et al. (2003) cannot be applied to massive galaxies directly but needs to be improved in the sense that the inclination is important as long as the ram pressure is comparable to the pressure in the galactic plane.

## 5.2 What could be observed?

A prediction for observable gas surface density maps is given in Figs. 4 to 6. We want to emphasise one special aspect, namely the relation between the direction of the tail of stripped gas and the galaxy’s direction of motion. Consider, e.g., the following surface density maps (all at  $t = 200 \text{ Myr}$ ): Fig. 4, first line and first column; Fig. 5 second line and second column; and Fig. 6 first column. Also focus on contour lines of  $10^{-4} \text{ g cm}^{-2}$  and above, as it would be the case for “normal” HI observations. Now try to guess the galaxy’s direction of motion purely from these maps, from the direction of the tail. The answer is *not* that the galaxy is moving into the direction opposite to the tail, but in all cases the galaxy is moving towards the left. The reason for this strange appearance is simple for the two cases where the disc is seen edge-on: Going back to the rest frame of the galaxy, the ICM wind is blowing the stripped gas towards the right. The gas

from the upwind edge has to go a longer way to reach a certain distance to the galaxy in  $y$ -direction, whereas the gas from the downwind edge has a “head start”. Moreover, in the direct vicinity of the galaxy, the ICM wind is not blowing straight in  $y$ -direction, but it is flowing smoothly past the galaxy. This introduces velocity components in  $\pm x$  and  $\pm z$  direction. Therefore, for some time during the initial phase the tail of stripped gas appears to be in the “wrong” direction. For such cases, not even radial velocity information would help to determine the true direction of motion because this behaviour is governed completely by velocities perpendicular to the line-of-sight.

In the case of the map in Fig. 5, second line and second column, the reason is a different one. This galaxy is moving edge-on through the ICM, while we see it face-on. If we can determine the position of the galactic centre, e.g. from the stellar disc, we would see that the gas disc is stretched towards the top-right and compressed at the opposite side. But also this galaxy is moving towards the left. In this example, we can see the interaction between the galactic rotation and the ICM wind. In this map, the galaxy is rotating counter-clockwise. The side where the gas rotates parallel to the ICM wind is stripped more easily than the side where the gas rotates antiparallel to the wind. In later stages (further maps in the middle column of Fig. 5), we can see that the tail of stripped gas seems to be attached to the bottom side of the galaxy. Phookun & Mundy (1995) discussed the effects of combined stripping and rotation and concluded that in such a geometry the side where the gas rotates *into* the wind will be stripped more strongly because, as the relative velocity between the gas and the ICM is higher at that side, also the true ram pressure is higher at this side. Thus, the tail of stripped gas should be twisted towards this more strongly stripped side. This is just the opposite of what our simulations show. The relative velocity is higher at the side where the gas rotates into the wind, and also the ram pressure may be stronger there. But at this side the gas first has to be decelerated to zero velocity and then accelerated to get stripped. At the opposite side, the gas is already moving in wind direction and, hence, it seems easier to strip it there.

In all cases discussed here, deep HI observations that reveal the low density extension of the tail or, for supersonic cases, the observation of a bow shock could help to determine the true direction of motion.

## 5.3 Application to cluster galaxies

The strongest limitation of our approach is the use of a constant ICM wind, which is not a good model for galaxies that traverse the cluster centre. Nonetheless, some of our results are applicable to real cluster galaxies.

According to our simulations, the mass loss is similar for galaxies that do not move close to edge-on also in initial phase of stripping. Therefore, even if galaxies are exposed to strong ram pressures for a short period only, only those galaxies that are close to edge-on can be protected against stripping by their inclination. Most galaxies should suffer severe stripping in cluster centres.

Although the mass loss from galaxies in low ram pressure environments such as cluster outskirts is small, Roediger & Hensler (2005) found that still the gas discs are truncated at  $\sim 15$  to 20 kpc. While this work was restricted

to face-on geometries, we found that this is also true for all non-close-edge-on geometries. Thus, ram pressure stripping of massive galaxies may also play a role in cluster outskirts. Observational evidence for the “pre-processing” of galaxies in low-density environments (see also Fujita 2004) arises from the detection of HI deficient galaxies (Solanes et al. 2001) and passive spirals (Goto et al. 2003) in cluster outskirts.

The duration of the intermediate phase, which is the phase where a substantial amount of gas that will be stripped eventually, is still bound to the galaxy, is independent of inclination. Therefore, we expect that if the ICM wind strength decreases during this phase, as it could be the case for galaxies passing cluster centres, a substantial amount of the stripped gas will still be bound to the galaxy and will fall back to the disc. This effect was found by Vollmer et al. (2001) in their sticky particle simulations. They also found that the amount of gas that falls back into the galaxy increases with inclination. It will be interesting to compare this feature with hydrodynamical simulations of a cluster passage.

If the ICM wind decreases during the intermediate phase, it leaves behind a gas disc with a strong asymmetry in the outer parts. Differential rotation should smear out this asymmetry on a few galactic rotation timescales, resulting in a gas disc with a steepened gas density profile in the outer parts. A similar feature has been observed recently by Koopmann et al. (2005) in the H $\alpha$  discs of Virgo spirals. We suggest that this feature could be caused by the scenario we just described.

## 6 SUMMARY

We have presented 3D hydrodynamical simulations of ram pressure stripping of massive disc galaxies. We concentrated on the influence of the inclination angle between the galactic rotation axis and the galaxy’s direction of motion.

We find that the inclination angle has a weak effect on the mass loss from the gas disc as long as the galaxy is not moving close to edge-on. We can explain this behaviour analytically by comparing the effective ram pressure with the component of the gravitational restoring force in wind direction. From simulations of dwarf galaxies, Marcolini et al. (2003) concluded that the inclination angle does not play a role as long as the ICM ram pressure is not comparable to the central disc pressure,  $p_0$ . For  $p_{\text{ram}} < p_0$  hardly any gas would be lost, and for  $p_{\text{ram}} > p_0$  the gas disc would be stripped completely for all inclinations. We refine this result in the sense that for massive galaxies it is not sufficient to compare the central disc pressure with  $p_{\text{ram}}$ , but the pressure profile along the galactic plane must be used for this comparison. This leads to a larger range of ram pressures for which the inclination angle plays a role.

We have also studied the phases of the ICM-ISM interaction and found that for all non-edge-on geometries the stripping proceeds in a remarkably similar fashion: First, during the instantaneous stripping phase, the outer part of the gas disc is pushed towards the downstream direction. Then follows the intermediate phase which is needed to unbind the stripped gas from the galactic potential. Finally,

during the continuous stripping phase the gas disc continues to lose gas at a small rate of  $\sim 1M_{\odot} \text{ yr}^{-1}$ .

In addition to the mass loss, we have studied the asymmetrical structure introduced in the remaining gas discs of inclined galaxies.

We have also presented projected gas density maps for several simulation runs. We have demonstrated that in moderately deep HI observations the tail of stripped gas does not necessarily point in a direction opposite to the galaxy’s direction of motion. Therefore, the observation of a galaxy’s gas tail may be misleading about the galaxy’s direction of motion. Deep HI observations or additional observations of, e.g., a bow shock may be essential.

## ACKNOWLEDGEMENTS

We acknowledge the support by the DFG grant BR 2026/3 within the Priority Programme “Witnesses of Cosmic History” and the supercomputing grants NIC 1927 and 1658 at the John-Neumann Institut at the Forschungszentrum Jülich. Some of the simulations were produced with STELLA, the LOFAR BlueGene/L System.

The results presented were produced using the FLASH code, a product of the DOE ASC/Alliances-funded Center for Astrophysical Thermonuclear Flashes at the University of Chicago.

We gratefully acknowledge fruitful and helpful discussions with Joachim Köppen and Gerhard Hensler.

## APPENDIX A: RESOLUTION COMPARISON

We have performed some of our simulation runs with two different resolutions to verify that our results are resolution independent. In Figs. A1 and A2, we repeat slices through the simulation box corresponding to Figs. 2 and 3, but for the lower resolution of 500 pc. In the higher resolution runs, the stripped gas fragments more than in the low resolution runs, but the overall structure is very similar for both resolutions.

In Fig. A3, we repeat Fig. 7 but for the low resolution case. Here the numerical diffusion problem in the inner part as explained in Sect. 4.3 occurs in a larger region in the inner part. Aside from this, the characteristics of the profiles are very similar for the two resolutions.

In Fig. A4, we demonstrate that the disc radius and mass evolution are nearly independent of resolution. Even the mass loss rate in the continuous stripping phase is very similar. This is due to the fact that the mass loss is dominated by the largest KH-modes, which are also resolved in the lower resolution runs.

We conclude that our simulations use a sufficient resolution.

## REFERENCES

- Abadi M. G., Moore B., Bower R. G., 1999, MNRAS, 308, 947
- Binney J., Tremaine S., 1987, Galactic Dynamics. Princeton University Press, Princeton, New Jersey
- Burkert A., 1995, ApJ, 447, 25

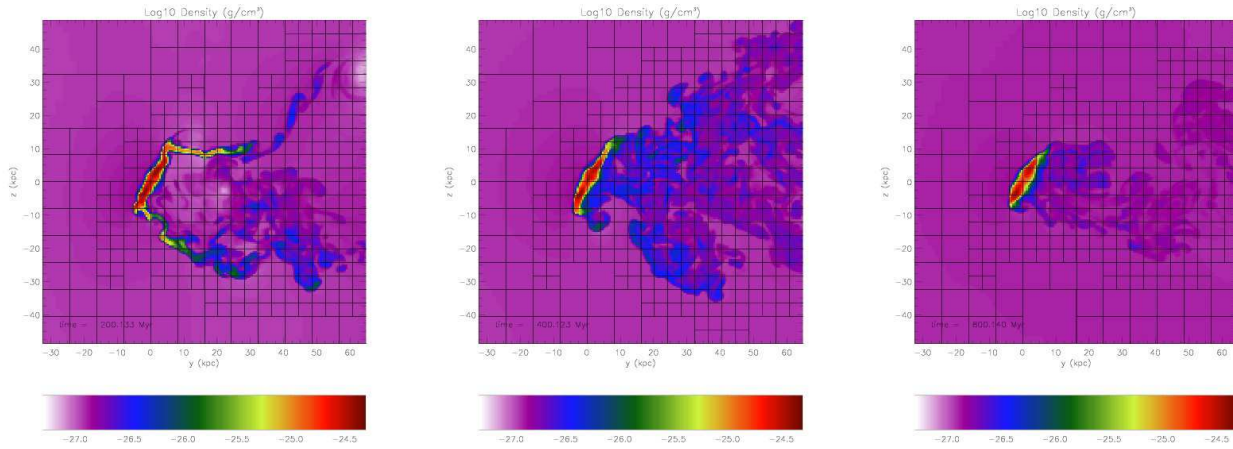


**Figure A1.** Same as Fig. 2, but for lower resolution ( $\Delta x = 500$  pc).

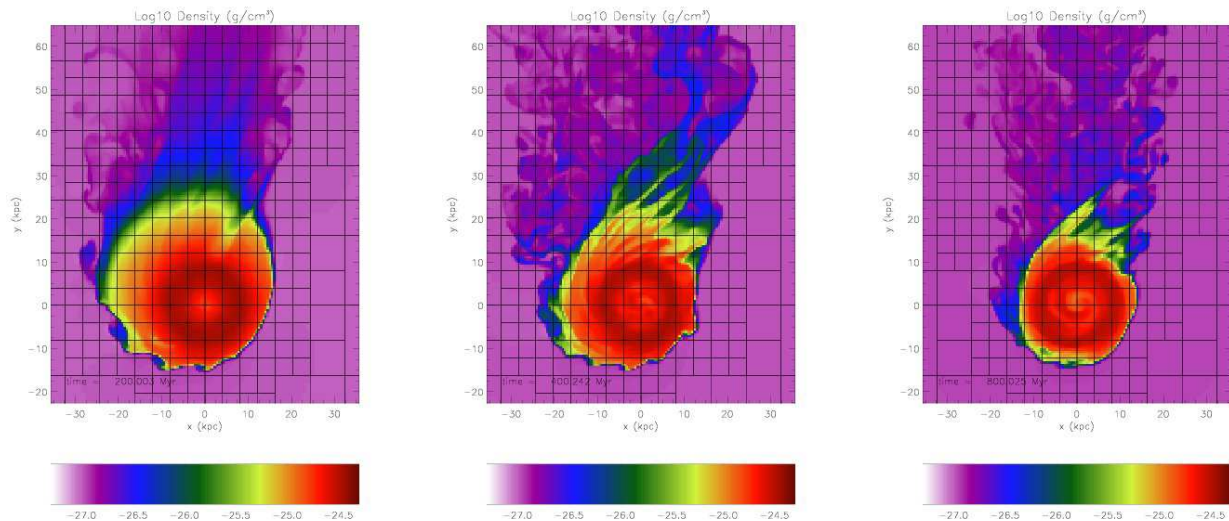


**Figure A2.** Same as Fig.3, but for lower resolution run ( $\Delta x = 500$  pc).

Cayatte V., Kontanyi C., Balkowski C., van Gorkom J. H., 1994, *AJ*, 107, 1003  
 Cayatte V., van Gorkom J. H., Kotanyi C., 1990, *AJ*, 100, 604  
 Fryxell B., Olson K., Ricker R., Timmes F. X., Zingale M., Lamb D. Q., MacNeice P., Rosner R., Truran J. W., Tufo H., 2000, *ApJS*, 131, 273  
 Fujita Y., 2004, *PASJ*, 56, 29  
 Goto T., Okamura S., Sekiguchi M., Bernardi M., Brinkmann J., Gómez P. L., Harvanek M., Kleinman S. J., Krzesinski J., Long D., Loveday J., Miller C. J., Nielsen E. H., Newman P. R., Nitta A., Sheth R. K., Snedden S. A., Yamauchi C., 2003, *PASJ*, 55, 757  
 Goto T., Yamauchi C., Fujita Y., Okamura S., Sekiguchi M., Smail I., Bernardi M., Gomez P. L., 2003, *MNRAS*, 346, 601  
 Gunn J. E., Gott J. R., 1972, *ApJ*, 176, 1  
 Hernquist L., 1993, *ApJS*, 86, 389  
 Kenney J. D. P., Koopmann R. A., 1999, *AJ*, 117, 181

Kenney J. D. P., Koopmann R. A., 2001, in Hibbard J. E., Rupen M. P., van Gorkom J. J., eds, *Gas and Galaxy Evolution Vol. 240 of ASP Conf. Ser.*, Environmental effects on gas and star formation in virgo cluster spiral and peculiar galaxies. ASP, San Francisco, p. 577  
 Kenney J. D. P., van Gorkom J. H., Vollmer B., 2004, *AJ*, 127, 3361  
 Koopmann R. A., Haynes M. P., Catinella B., 2005, *AJ*, in press, astro-ph/0510374  
 Koopmann R. A., Kenney J. D. P., 1998, *ApJ*, 497, 75L  
 Koopmann R. A., Kenney J. D. P., 2004a, *ApJ*, 613, 866  
 Koopmann R. A., Kenney J. D. P., 2004b, *ApJ*, 613, 851  
 Marcolini A., Brighenti F., A.D'Ercole 2003, *MNRAS*, 345, 1329  
 Mihos J. C., 2004, in Mulchaey J. S., Dressler A., Oemler A., eds, *Clusters of Galaxies: Probes of Cosmological Structure and Galaxy Evolution Vol. 3 of Carnegie Observatories Astrophysics Series*, Interactions and Mergers of Cluster Galaxies. Cambridge Univ. Press, Cambridge,

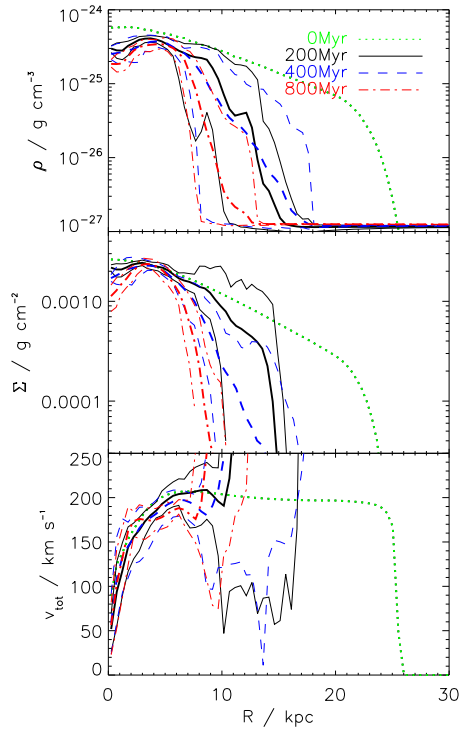


**Figure A3.** Same as Fig. 7, but for low resolution run.

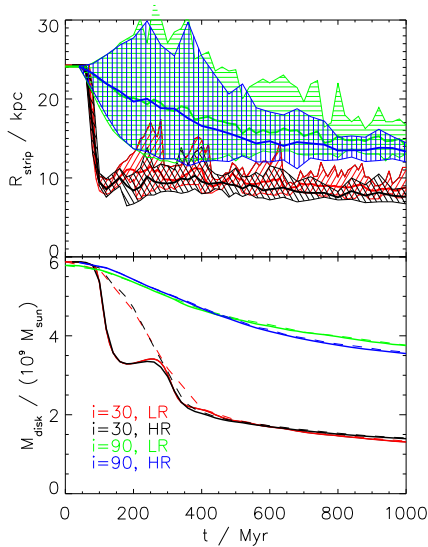


**Figure A4.** Comparison of disc radius and mass evolution for two different resolutions. For medium ram pressure, inclination  $30^\circ$ .

p. 278

- Miyamoto M., Nagai R., 1975, PASJ, 27, 533  
 Moore B., Katz N., Lake G., Dressler A., Oemler A., 1996, Nature, 379, 613  
 Moore B., Lake G., Katz N., 1998, ApJ, 495, 139  
 Moore B., Lake G., Quinn T., Stadel J., 1999, MNRAS, 304, 465  
 Mori M., Burkert A., 2000, ApJ, 538, 559

- Nulsen P. E. J., 1982, MNRAS, 198, 1007  
 Phookun B., Mundy L. G., 1995, ApJ, 453, 154  
 Pimblett K. A., 2003, Publications of the Astronomical Society of Australia, 20, 294  
 Quilis V., Moore B., Bower R., 2000, Science, 288, 1617  
 Roediger E., 2005, PhD thesis, Christian-Albrechts-Universität zu Kiel  
 Roediger E., Hensler G., 2005, A&A, 433, 875  
 Schulz S., Struck C., 2001, MNRAS, 328, 185  
 Solanes J. M., Manrique A., García-Gómez C., González-Casando G., Giovanelli R., Haynes M. P., 2001, ApJ, 548, 97  
 Vollmer B., 2003, A&A, 398, 525  
 Vollmer B., Beck R., Kenney J. D. P., van Gorkom J. H., 2004, AJ, 127, 3375  
 Vollmer B., Braine J., Balkowski C., Cayatte V., Duschl W. J., 2001, A&A, 374, 824  
 Vollmer B., Cayatte V., Balkowski C., Duschl W. J., 2001, ApJ, 561, 708  
 Vollmer B., Cayatte V., Boselli A., Balkowski C., Duschl W. J., 1999, A&A, 349, 411  
 Vollmer B., Marcelin M., Amram P., Balkowski C., Cayatte V., Garrido O., 2000, A&A, 364, 532

This paper has been typeset from a  $\text{\TeX}$ / $\text{\LaTeX}$  file prepared by the author.